

IMPROVING ROBUSTNESS IN PRINTED SIDE COMMUNICATIONS USING HIGHER ORDER STATISTICS

Paulo Vinicius Koerich Borges and Joceli Mayer

LPDS - Dept. of Electrical Engineering - Federal University of Santa Catarina, SC, Brazil

E-mail: vini@ieec.org, mayer@eel.ufsc.br

ABSTRACT

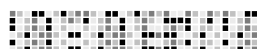
This paper uses higher order statistical moments to improve the detection in systems which transmit side information through the print and scan channel, such as 2-D bar codes and text luminance watermarking. When these systems print symbols using halftoning, symbol detection can be performed by evaluating second, third, and fourth order statistical moments of the transmitted symbol, in addition to the average luminance level. A print and scan channel model is described. The relationship between the modulated luminance and the higher order moments of a halftone image is analyzed. The detection error rate is reduced by merging the different moments into a single metric. Experiments validate the analyses and the applicability of the method.

Index Terms— Higher order statistics, 2-D bar codes, hardcopy watermarking, print-scan.

1. INTRODUCTION

Despite of the advances on video, telephony and Internet based communications, communication over paper is still an essential mean of conveying information. In addition to regular text and images, paper communications include, for example, bar codes and data hiding techniques, i.e., hardcopy watermarking.

Regarding bar codes, multi-level two-dimensional (2-D) bar codes [1, 2] have gained increased attention in the past few years. Instead of representing information with only black and white symbols, multi-level codes use gray levels to increase the bit rate, as illustrated in Fig. 1(a), acting as a higher capacity version of 1-D bar codes.



(a) Multi-level 2-D bar code.

SIGNAL PROCESSING

1 0 0 1 1 0 0 0 1 1 1 0 1 0 0 1

(b) Example of text watermarking through luminance modulation.

Fig. 1: Illustration of side communications over paper.

In the context of hardcopy watermarking, an important class of algorithms is that of luminance alteration of text (LAT) [3, 4, 5], which slightly modifies the luminance of text characters to embed information. This modification, which depends on the message to be inserted, can be set perceptually transparent and can still be detected after scanning. An example of this technique is given in Fig. 1(b), where the characters are visibly modified to illustrate the process.

This work was supported by CNPq, Proc. No 141078/2004-9.

The systems described above print symbols with different luminances, depending on the message to be transmitted. They usually perform the detection using the average amplitude [1, 5] or spectral characteristics [4] of the region of interest as a detection metric. However, because halftoning is usually employed in the printing process, other statistics of the received signal can also be used. In this scenario, the contributions presented in this work are listed as follows. (i) The use of higher order statistical moments, such as variance, skewness and kurtosis in the detection process is proposed. (ii) To justify the use of these new metrics, a print and scan (PS) channel model is described, which includes characteristics of the halftoning process. (iii) The relationship between the average luminance and the higher order statistics of a halftone region is analyzed, both before and after the PS process. (iv) To provide more robustness to the PS distortions, combining the different metrics into a single metric is proposed, decreasing the detection error probabilities and allowing that previously proposed metrics [4, 5] be combined with the ones proposed in this paper. To combine the metrics, the Bayes classifier is adopted in this work. (v) Experiments validate the analyses and the proposed modifications.

This paper is organized as follows. Section 2 briefly discusses halftoning algorithms and describes a PS model. Section 3 analyzes the relationship between the different moments and the average luminance before PS, whereas Section 4 performs a similar analysis considering the PS distortions. Experimental results are presented in Section 5, followed by conclusions in Section 6.

2. THE PRINT AND SCAN CHANNEL

This section describes the halftoning process, which takes place prior the printing. This description is focused on ordered dithering halftoning. Although spectral characteristics depend on the halftone used [6], characteristics of the higher order moments are similar for different types of halftoning algorithms.

Let s be a digital image of size $M \times N$ with $L + 1$ levels in the range $[0,1]$, where $\mathbf{0}$ represents **white** and $\mathbf{1}$ represents **black**. A halftoned image (binary) b is generated from s , using the ordered dithering halftoning algorithm. The output of this method depends on the size and on the coefficients of the *dithering matrix* D of size $J \times J$, where each coefficient represents a threshold level. The coefficient values in D are approximately uniformly distributed [6]. Each coefficient takes a value from the set $\{0, 1/L, 2/L, \dots, 1\}$. The binary output image b is given by an element-by-element thresholding operation between the pixels $s(m, n)$ and the coefficients $D(m, n)$. In general, $J \ll M$ and $J \ll N$. The input-output relationship of ordered dithering can be mathematically described by:

$$b(m, n) = \begin{cases} 0 & \text{if } s(m, n) \geq D(m \bmod J, n \bmod J) \\ 1 & \text{otherwise} \end{cases} \quad (1)$$

where the output ‘0’ represents a white pixel (do not print a dot), and ‘1’ represents a black pixel (print a dot).

Analytical models of the PS channel have been presented in the literature [1, 2]. In addition to the geometric distortions (possible rotation, re-scaling, and cropping), those PS models assume that the process can be modeled by low-pass filtering, the addition of Gaussian noise, and non-linear gains, such as brightness and gamma alteration. In the following a modified PS channel model is described, which in contrast to other existing models, includes the halftone signal to justify the use of higher order moments to decode information.

The digital scanned image y is represented by

$$y(m, n) = g_s \left\{ \left\{ g_{pr} [b(m, n)] + \eta_1(m, n) \right\} * h(m, n) \right\} + \eta_3(m, n), \quad (2)$$

where b is the halftoned image generated from the original image s , as described in (1). η_1 represents printing noise due to microscopic ink and paper imperfections. The noise η_3 combines illumination and CCD electronic noise [1], as well as the quantization noise due to A/D. The operator $*$ represents convolution and the linear system h is a low-pass filter combining the point-spread functions of the printer and of the scanner. In the printing process, blurring occurs due to toner or ink spread [7]. In the scanning process, the low-pass effect is due to the optics and the motion blur caused by the interactions between adjacent CCD arrays elements [1].

The term $g_{pr}(\cdot)$ in (2) represents a gain in the printing process. In practice, when toner or black ink particles are applied over the paper, they do not present a null reflectance, causing a luminance gain to the printed image. This distortion is described by $g_{pr}(m, n) = \alpha(m, n)b(m, n)$, where α is a gain affecting the black elements of b . $\alpha(m, n)$ is modeled as constant for a small region (an area corresponding to one 2-D bar code symbol, for example), but it does vary throughout a full page due to non-constant printer toner distribution.

The term $g_s(\cdot)$ represents the response of scanners, which vary depending on the device. They may cause a non-linear gain to the scanned image, represented by $g_s(m, n) = [x(m, n)]^\phi$ as reported in results presented in [1].

3. EFFECTS INDUCED BY THE HALFTONE

The quantization due to halftoning affects the variance, the skewness, and the kurtosis of a halftoned region, according to the input luminance. This characteristic is demonstrated in the following.

The variance of a halftone block b_0 of size $J \times J$ is given by:

$$\sigma_{b_0}^2 = \frac{1}{J^2} \sum_{m=1}^J \sum_{n=1}^J [b_0(m, n) - \bar{b}_0]^2 \quad (3)$$

$$= \frac{1}{J^2} \sum_{m=1}^J \sum_{n=1}^J b_0(m, n)^2 - 2b_0(m, n)\bar{b}_0 + \bar{b}_0^2, \quad (4)$$

where $b_0(m, n) \in \{0, 1\}$, $\bar{b}_0 = (1/J^2) \sum_{m=1}^J \sum_{n=1}^J b_0(m, n)$ and J^2 is the number of coefficients in the dithering matrix. Since $b_0(m, n) \in \{0, 1\}$, $b_0^2(m, n) = b_0(m, n)$, and (4) can be written as

$$\sigma_{b_0}^2 = \bar{b}_0 - 2\bar{b}_0\bar{b}_0 + \bar{b}_0^2 = \bar{b}_0 - \bar{b}_0^2. \quad (5)$$

Similar analyses are performed for the skewness and for the kurtosis.

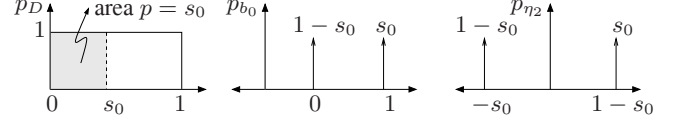


Fig. 2: From left to right: distribution assumed for the coefficients in D ; distribution of b_0 ; distribution of η_2 .

The skewness measures the degree of asymmetry of a distribution around its mean. It is zero when the distribution is symmetric, positive if the distribution shape is more spread to the right and negative if it is more spread to the left [8]. The skewness of a halftone block b_0 of size $J \times J$ is given by:

$$\gamma_{1b_0} = \frac{\frac{1}{J^2} \sum_{m=1}^J \sum_{n=1}^J [b_0(m, n) - \bar{b}_0]^3}{\sigma_{b_0}^3} = \frac{\bar{b}_0 - 3\bar{b}_0^2 + 2\bar{b}_0^3}{(\bar{b}_0 - \bar{b}_0^2)^{3/2}} \quad (6)$$

The kurtosis measures the relative flatness or peakedness of a distribution about its mean, with respect to a normal distribution [8]. The kurtosis of a halftone block b of size $J \times J$ is given by:

$$\begin{aligned} \gamma_{2b_0} &= \frac{\frac{1}{J^2} \sum_{m=1}^J \sum_{n=1}^J [b_0(m, n) - \bar{b}_0]^4}{\sigma_{b_0}^4} - 3 \\ &= \frac{\bar{b}_0 - 4\bar{b}_0^2 + 6\bar{b}_0^3 - 3\bar{b}_0^4}{(\bar{b}_0 - \bar{b}_0^2)^2} - 3 \end{aligned} \quad (7)$$

To derive $\sigma_{b_0}^2$, γ_{1b_0} and γ_{2b_0} as a function of the input luminance $s(m, n)$, $b_0(m, n)$ must be generated from a constant gray level region, that is, $s(m, n) = s_0$, $m, n = 1, \dots, J$, where s_0 is a constant. Assuming that D is approximately uniformly distributed as illustrated by p_D in Fig. 2, the probability p of $b_0(m, n) = 1$, which is $\Pr[s_0 > D(m, n)]$, is given by

$$p = \Pr[s_0 > D(m, n)] = \frac{1}{J^2} \sum_{b_0(m, n)=1} b_0(m, n) = \bar{b}_0 = s_0 \quad (8)$$

illustrated by the area p in p_D in Fig. 2. Substituting this result into (5), (6) and (7), yields $\sigma_{b_0}^2 = s_0 - s_0^2$, $\gamma_{1b_0} = \frac{s_0 - 3s_0^2 + 2s_0^3}{(s_0 - s_0^2)^{3/2}}$ and $\gamma_{2b_0} = \frac{s_0 - 4s_0^2 + 6s_0^3 - 3s_0^4}{(s_0 - s_0^2)^2}$, which represent respectively the variance, the skewness, and the kurtosis of a halftoned block that represents a region of constant luminance s_0 .

Because $\sigma_{b_0}^2$, γ_{1b_0} and γ_{2b_0} depend on s_0 , these moments can be used as detection metrics in text watermarking and multi-level bar codes. The variance, for example, is maximum in the middle of the input range ($s_0 = 0.5$), where the black and white areas are approximately equal. Regarding the skewness, it is equal to zero when $s_0 = 0.5$ and the distribution of b_0 is symmetric, represented by two peaks of equal probabilities. The symmetric peaks also flatten the distribution of b_0 , minimizing the kurtosis. When $s_0 < 0.5$, b_0 is composed of more white dots than black dots, leaning the distribution of b_0 to the left and causing a positive skewness. The opposite occurs when $s_0 > 0.5$, causing a negative skewness. These effects are illustrated in the experiments section.

4. EFFECTS INDUCED BY THE PS CHANNEL

The metrics described in (5), (6) and (7) are distorted by the low-pass characteristic and the additive noise of the PS channel. Considering these distortions, σ_y^2 , γ_{1y} and γ_{2y} (statistical moments after PS) are derived in the following. For simplicity, the (m, n) coordinate system is mapped to an one dimensional notation.

In the model in (2), it is possible to decompose b into a constant term \bar{b} added to a noise term η_2 , such that $b(n) = \bar{b} + \eta_2(n)$. The noise η_2 is zero-mean with variance given by $\sigma_{\eta_2}^2 = \sigma_b^2$, and distribution $\eta_2 \in \{-s_0, 1 - s_0\}$, as illustrated by p_{η_2} in Fig. 2.

Approximating ϕ to 1 in the gain g_s in (2) and assuming that b is generated from a constant gray level region, that is, $s(n) = s_0 = \bar{b}$, (2) can be written as

$$y(n) = \{\alpha[s_0 + \eta_2(n)] + \eta_1(n)\} * h(n) + \eta_3(n), \quad (9)$$

The term α represents a gain (see g_{pr} in (2)) that varies slightly throughout a full page due to non-uniform printer toner distribution. Due to its slow rate of change, α is modeled as constant in n but it varies with each realization i satisfying $\alpha \sim \mathcal{N}(\mu_\alpha, \sigma_\alpha^2)$, where i represents the i -th symbol of a 2-D bar code, for example.

Due to the nature of the noise (discussed in Section 2) and based on experimental observations, η_1 and η_3 can be generally modeled as zero-mean mutually independent Gaussian noise [1, 2].

The sample variance of a scanned symbol y of size N is given by

$$\sigma_y^2 = \frac{1}{N} \sum_{n=1}^N [y(n) - \bar{y}]^2 \quad (10)$$

Considering the statistical characteristics assumed for the noise terms in (9), a statistical analysis shows that the result of the expected value of (10) as a function of s_0 can be approximated to

$$\mu_{\sigma_y^2} = (\mu_\alpha^2 + \sigma_\alpha^2) \sigma_{\eta_2}^2 r_h(0) + \sigma_{\eta_1}^2 r_h(0) + \sigma_{\eta_3}^2 \quad (11)$$

where $\sigma_{\eta_2}^2 = s_0 - s_0^2$ and $r_h(l)$ represents the autocorrelation function of the impulse response of h . Similar analyses are performed for the skewness γ_{1y} and for the kurtosis γ_{2y} , which yield:

$$\mu_{\gamma_{1y}} = \frac{(3\sigma_\alpha^2 \mu_\alpha + \mu_\alpha^3)[(1-s_0)(-s_0)^3 + (1-s_0)^3 s_0] r_h^2(0)}{(\mu_{\sigma_y^2})^{3/2}} \quad (12)$$

$$\begin{aligned} \mu_{\gamma_{2y}} = & \frac{1}{(\mu_{\sigma_y^2})^2} \left((3\sigma_\alpha^4 + 6\sigma_\alpha^2 \mu_\alpha^2 + \mu_\alpha^4)[(1-s_0)(-s_0)^4 \right. \\ & + (1-s_0)^4 s_0] r_h^2(0) + 6(\sigma_\alpha^2 + \mu_\alpha^2) \sigma_{\eta_1}^2 \sigma_{\eta_2}^2 r_h^2(0) \\ & + 6(\sigma_\alpha^2 + \mu_\alpha^2) \sigma_{\eta_2}^2 \sigma_{\eta_3}^2 r_h(0) + 3\sigma_{\eta_1}^4 r_h^2(0) \\ & \left. + 6\sigma_{\eta_1}^2 \sigma_{\eta_3}^2 r_h(0) + 3\sigma_{\eta_3}^4 \right) - 3 \end{aligned} \quad (13)$$

To reduce the detection error rate, it is possible to combine the average, variance, skewness and kurtosis of a received symbol into a single metric. In this work, the Bayes classifier [9] is employed to combine the metrics, although other classifiers can be used [9]. Although some detection metrics have better performance than others, because all the first four statistical moments are useful to separate classes, combining them increases the distance between classes, and consequently reduces the detection error rate [9], at the expense of increasing computational complexity. It is also possible to combine useful spectral or other non-statistical metrics, although this is not

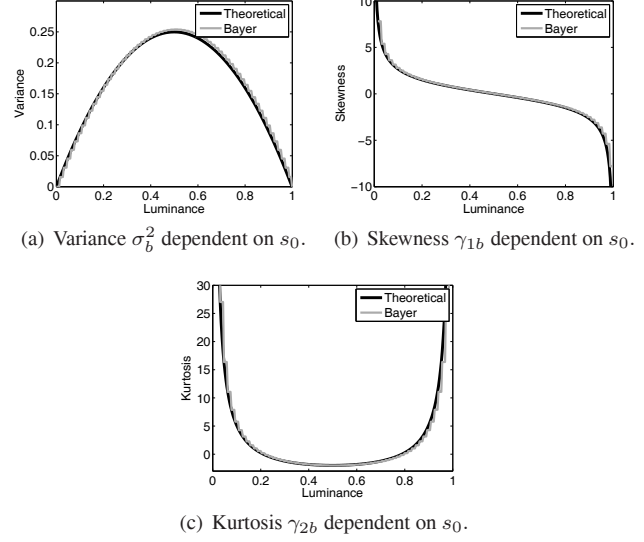


Fig. 3: Half-tone statistics dependent on the luminance s_0 , before PS.

discussed in this paper.

5. EXPERIMENTS

The experiments were conducted with printers HP IJ-855C, HP IJ-870Cxi and HP LJ-1100, and scanners Genius HR6X, HP 2300C and HP SJ-5P. The printing and scanning resolutions were set to 300 dots/inch and pixels/inch, respectively.

In the first experiment, the effect of a symbol variance level that depends on the input modulated luminance is illustrated in Fig. 3(a), where two curves are presented. The black curve ('Theoretical') represents the theoretical variance determined in (5). The gray curve ('Bayer') represents the variance of a halftoned block (before PS) generated using the Bayer dithering matrix [10]. Similar experiments are presented regarding the skewness and the kurtosis, as shown in Figs. 3(b) and 3(c). These figures illustrate that the analyses of Section 3 are in accordance with the results obtained from a practical halftoning matrix.

The second experiment illustrates the validity of the channel model described in Section 2 and the expected values of the higher order moments as a function of the input modulated luminance, determined analytically in Section 4. The effect of a printed and scanned variance level that depends on the input luminance is illustrated in Fig. 4(a), where two curves are presented. The black curve ('Theoretical') represents the theoretical variance determined in (11). The gray curve ('Experimental') represents the variance of actual printed and scanned blocks. Similar experiments are presented regarding the skewness and the kurtosis determined in (12) and (13), as shown in Figures 4(b) and 4(c), respectively.

In the third experiment a multi-level 2-D bar code is printed with a sequence of 56000 symbols with four possible luminance levels (2 bits/symbol) drawn from the alphabet $\{0.08, 0.34, 0.65, 0.95\}$. Optimum values for the alphabet depend on the PS devices used, as discussed in [1]. The size of each symbol is 8×8 pixels, corresponding to the size of one halftone block. Table 1 shows the obtained bit error rates when performing the detection using two suggested metrics (average and skewness) separately. This table also presents

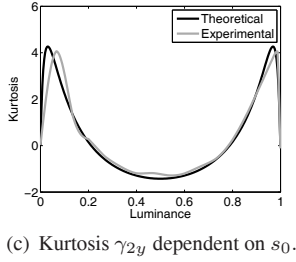
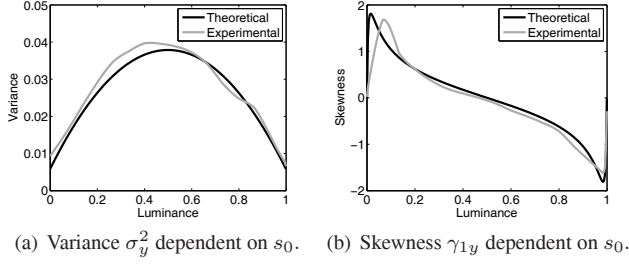


Fig. 4: Higher order statistics dependent on the luminance, after PS.

Table 1: Experimental error rates for 2-D bar codes.

Metric	Number of Errors	Error Rate
Average (μ)	667	1.19×10^{-2}
Kurtosis (γ_2)	1860	3.32×10^{-2}
Comb. (μ, σ^2)	114	2.04×10^{-3}
Comb. (μ, γ_1)	259	4.63×10^{-3}
Comb. (μ, σ^2, γ_1)	50	8.93×10^{-4}
Comb. ($\mu, \sigma^2, \gamma_1, \gamma_2$)	22	3.93×10^{-4}

the results of combining the metrics with the Bayes classifier, illustrating a smaller error rate. The variance and the kurtosis cannot be used alone because they are symmetric around the middle of the luminance range.

The fourth experiment implemented the text hardcopy watermarking system [4, 5], which embeds data by performing modifications in the luminances of characters, respecting a perceptual transparency requirement. A sequence of 15180 characters (as in ‘abcdef...’) is printed and scanned. The font type tested was ‘Arial’, size 12. The luminances of the characters were randomly modified to {0.95, 0.84} with equal probability, where 0.95 corresponds to bit 0 and 0.84 corresponds to bit 1. To determine to which class (bit 0 or bit 1) each received character belongs to, the four metrics were used. The resulting obtained error rates are given in Table 2. Illustrations

Table 2: Experimental error rates for text watermarking.

Metric	Number of Errors	Error Rate
Average (μ)	157	1.03×10^{-2}
Variance (σ^2)	144	9.48×10^{-3}
Skewness (γ_1)	280	1.84×10^{-2}
Kurtosis (γ_2)	328	2.16×10^{-2}
Comb. (μ, σ^2)	14	9.22×10^{-4}
Comb. (μ, γ_1)	27	1.78×10^{-3}
Comb. (μ, σ^2, γ_1)	8	5.27×10^{-4}
Comb. ($\mu, \sigma^2, \gamma_1, \gamma_2$)	3	1.98×10^{-4}

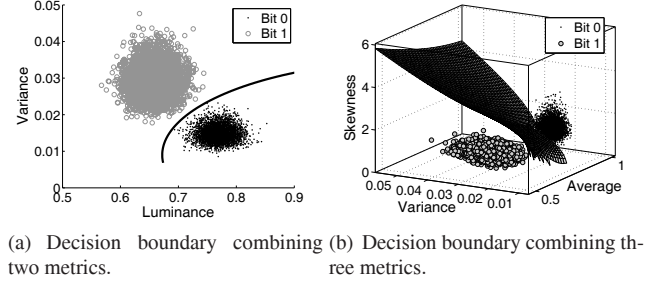


Fig. 5: Illustration of the use of the Bayes classifier.

of employing the Bayes classifier to combine metrics are given in Fig. 5(a) (μ, σ^2) and in Fig. 5(b) (μ, σ^2, γ_1).

6. CONCLUSIONS

This paper reduces the detection error rate of printed symbols in applications where the luminances of the symbols depend on a message to be transmitted through the PS channel. As a consequence of modifying the luminances, the halftoning in the printing process also modifies the higher order statistical moments of a symbol, such as the variance, the skewness and the kurtosis. Therefore, in addition to the average luminance, these moments are also used to detect a received symbol without the need of performing any modifications in the transmitting function. A PS channel model is presented. Analyses determining the relationship between the average luminance and the higher order moments of a halftoned image and of a PS image are presented, justifying the use of the new detection metrics. The experiments have illustrated the applicability of the new metrics and that a significant reduction of error rate is achieved when the metrics are combined into a single decision metric.

7. REFERENCES

- [1] N. D. Quintela and F. Pérez-González. “Visible encryption: Using paper as a secure channel.” In *Proc. of SPIE, USA*, 2003.
- [2] R. Vllan, S. Voloshynovskiy, O. Koval, and T. Pun, “Multilevel 2D bar codes: towards high capacity storage modules for multimedia security and management,” in *Proc. of SPIE*, 2005.
- [3] A. K. Bhattacharjya and H. Ancin, “Data embedding in text for a copier system,” *Proc. of IEEE ICIP*, Vol. 2, 1999.
- [4] R. Vllan, S. Voloshynovskiy, O. Koval, J. Vila, E. Topak, F. Deguillaume, Y. Rytsar and T. Pun, “Text data-hiding for digital and printed documents: theoretical and practical considerations” in *Proc. of SPIE, Elect. Imaging, USA*, 2006.
- [5] P. V. Borges and J. Mayer, “Document watermarking via character luminance modulation,” *IEEE ICASSP*, May 2006.
- [6] R. A. Ulichney, “Dithering with blue noise,” in *Proc. of IEEE*, Vol. 76, No. 1, 1988.
- [7] M. Norris, E. B. Smith “Printer modeling for document imaging,” *Proc. Int’l Conf. Imaging Sci., Systems and Tech.*, 2004.
- [8] D. Manolakis, V. Ingle, S. Kogon *Statistical and Adaptive Signal Processing*, McGraw-Hill, 2000.
- [9] S. Theodoridis, K. Koutroumbas, *Pattern Recog.*, AP, 2006.
- [10] B.E. Bayer, “An Optimum Method for Two-Level Rendition of Continuous Tone Pictures,” in *IEEE Int’l Conf. on Comm.*, 1973.